ELSEVIER

Materials Science and Engineering A 394 (2005) 43–52

MATERIALS SCIENCE & ENGINEERING A

www.elsevier.com/locate/msea

NiAl bond coats made by a directed vapor deposition approach

Z. Yu*, D.D. Hass, H.N.G. Wadley

Department of Materials Science and Engineering, University of Virginia, 116 Engineer's Way, Charlottesville, VA 22904, USA

Received 21 July 2004; received in revised form 28 October 2004

Abstract

Intermetallic, nickel aluminide alloys are widely used as bond coat materials in thermal barrier coating systems applied to nickel base super alloy components. They are usually synthesized by a solid-state reaction–diffusion heat treatment following the chemical vapor deposition of aluminum on the nickel rich substrate. Here, an electron beam directed vapor deposition (EB-DVD) technique is used to simultaneously evaporate nickel and aluminum and then reactively deposit NiAl bond coats that are structurally and chemically homogeneous and well bonded to the superalloy substrate. The approach utilizes individual nickel and aluminum sources placed within a rarefied helium gas jet with flow conditions that promote vapor phase intermixing. By adjusting the electron beam current applied to each elemental source, we show that the coating layer composition can be precisely controlled. Fully dense, homogeneous, β-phase NiAl coating layers with a relatively sharp compositional interface with the substrate have been deposited. The extent of the substrate interdiffusion zone is controlled by the deposition conditions.

Keywords: Thermal barrier coating; Bond coat; NiAl; EB-DVD

1. Introduction

Thermal barrier coating (TBC) systems are widely used to provide thermal and oxidation protection to nickel base superalloy components used in gas turbine engines [1]. In these systems, a metallic bond coat is used to provide a strong, oxidation protection layer for the superalloy substrate. The bond coat's oxidation resistance is achieved by the use of sufficient aluminum to result in the formation of α-alumina upon high temperature oxygen exposure [2,3]. The temperature at the bond coat surface then governs the rate of oxidation. For internally cooled components, this temperature can be reduced by applying a low thermal conductivity ceramic layer to the bond coat. The durability of the resulting TBC system depends on the ability of a candidate bond coat alloy to form an α-alumina layer with minimal intermediate phase formation during oxidation, the adherence of the resulting alumina layer to the bond coat and the high temperature strength/creep resistance of the bond coat [2,4,5]. All these features are significantly affected by the bond coats composition.

Near equiatomic (β-phase) nickel aluminide alloys have a B2 crystal structure, a high melting point (approximately 1995 K) and a low density (approximately 5.9 g/cm^3). They have been shown to be highly resistant to oxidation [6] and corrosion [7], while maintaining structural integrity during thermal cycling. These characteristics have resulted in the widespread use of NiAl-based bond coats in TBC systems [8,9].

Several approaches have been utilized for NiAl coating fabrication. Early attempts employed pack cementation to create thick (>25 μm) coatings [10–12]. This process is schematically illustrated in Fig. 1. In this method, a nickel aluminide coating is formed by the interdiffusion of aluminum and nickel. The aluminum is supplied from the vapor phase by a chemical vapor reaction with solid-state aluminum sources in the pack. The deposition of Ni and Al multilayers followed by reaction–diffusion heat treatments was later explored as a method for synthesizing thin film nickel aluminides [13]. The multilayers were deposited by sequential electron beam evaporation [14] or sputtering [15,16] from separate aluminum

* Corresponding author. Tel.: +1 434 924 4084; fax: +1 434 982 5677.
E-mail address: zy4r@virginia.edu (Z. Yu).

0921-5093/$ – see front matter © 2004 Elsevier B.V. All rights reserved.
doi:10.1016/j.msea.2004.11.017

Report Documentation Page

Form Approved
OMB No. 0704-0188

1. REPORT DATE	2. REPORT TYPE	3. DATES COVERED
OCT 2004		**00-00-2004 to 00-00-2004**

4. TITLE AND SUBTITLE	5a. CONTRACT NUMBER
NiAl bond coats made by a directed vapor deposition approach	5b. GRANT NUMBER
	5c. PROGRAM ELEMENT NUMBER
6. AUTHOR(S)	5d. PROJECT NUMBER
	5e. TASK NUMBER
	5f. WORK UNIT NUMBER
7. PERFORMING ORGANIZATION NAME(S) AND ADDRESS(ES) **University of Virginia,Department of Materials Science and Engineering,116 Engineer's Way,Charlottesville,VA,22904-4745**	8. PERFORMING ORGANIZATION REPORT NUMBER
9. SPONSORING/MONITORING AGENCY NAME(S) AND ADDRESS(ES)	10. SPONSOR/MONITOR'S ACRONYM(S)
	11. SPONSOR/MONITOR'S REPORT NUMBER(S)

12. DISTRIBUTION/AVAILABILITY STATEMENT
Approved for public release; distribution unlimited

13. SUPPLEMENTARY NOTES
The original document contains color images.

14. ABSTRACT

15. SUBJECT TERMS

16. SECURITY CLASSIFICATION OF:			17. LIMITATION OF ABSTRACT	18. NUMBER OF PAGES	19a. NAME OF RESPONSIBLE PERSON
a. REPORT	b. ABSTRACT	c. THIS PAGE			
unclassified	**unclassified**	**unclassified**		**10**	

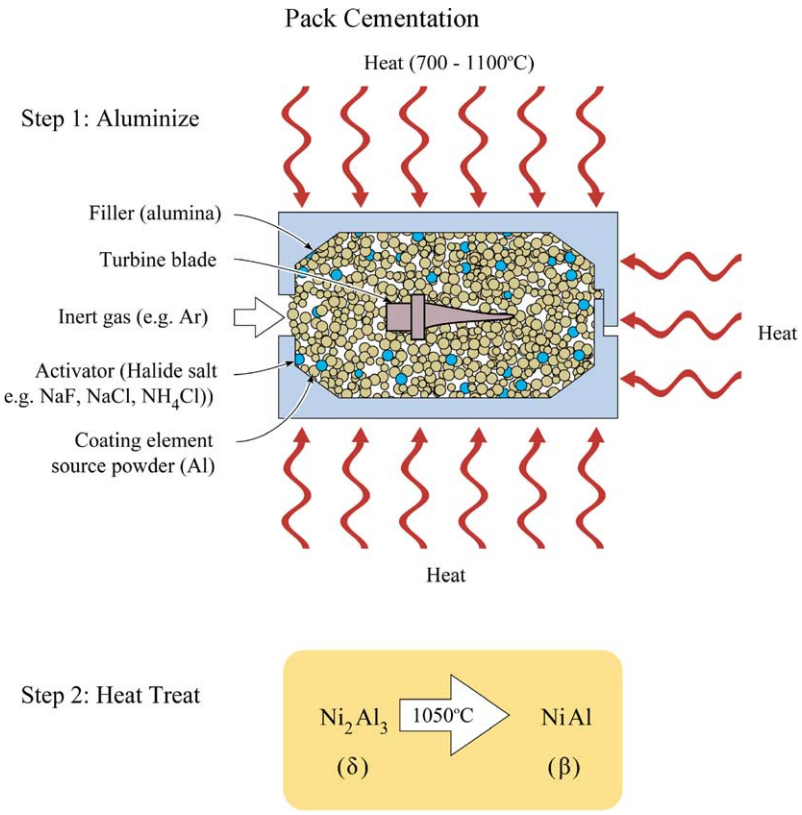

Fig. 1. A schematic illustration of the pack cementation process.

and nickel targets. More recently, low-activity chemical vapor deposition (CVD) has emerged as the preferred method of nickel aluminide coating fabrication [17–19]. This CVD process utilizes aluminum trichloride gas generated from outside the coating retort as the chemical precursor for aluminum and is schematically illustrated in Fig. 2.

Although these methods have successfully generated nickel aluminide layers, they complex synthesize processes and involve prolonged thermal exposure of the coating–substrate system to form the appropriate (B2) intermetallic NiAl phase. When further alloying (for example platinum) is required, an extra electroplating operation has to be added, increasing the complexity of the process and the opportunity for sample contamination [18,20]. These reaction–diffusion methods result in significant interdiffusion of the materials added to the surface and the underlying substrate alloy. This can compromise the coating if substrate alloy elements, such as W, Ta, Ti or S, are able to diffuse from the substrate into the nickel aluminide layer [4,18].

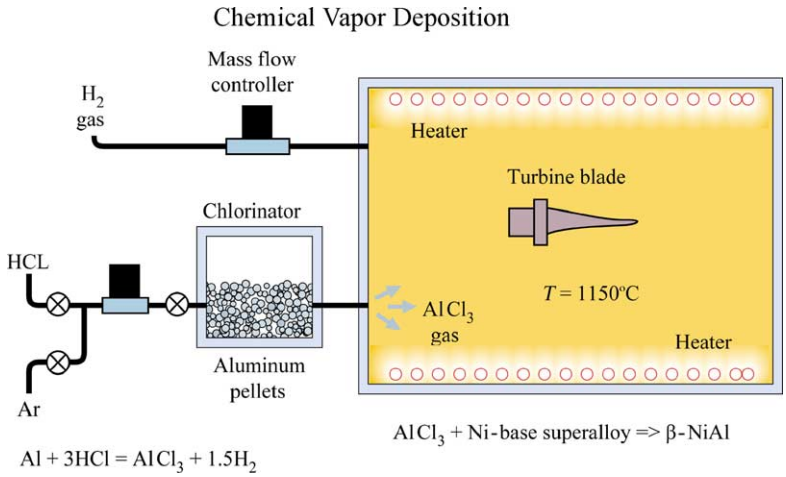

Fig. 2. A schematic illustration of the low-activity CVD process.

To address these difficulties, several groups have sought to co-evaporate the desired elements and to stoichiometrically deposit them on a substrate [21–24]. The goal was to grow an intermetallic layer directly without a requirement for a subsequent solid phase diffusion reaction step. Attempts to make such NiAl thin films using RF magnetron sputter deposition [21–23] and ion-assist sputter deposition [24] have been reported. In both approaches, NiAl compound targets or co-axial disk targets were used to obtain the required deposition composition coating. Both of these sputtering processes suffer from a low deposition rate (which prolongs the deposition time) and result in strictly line-of-sight coating which can result in some parts of a component having too thin (or no) coating.

Here, we explore a different thermal evaporation approach in which separate Ni and Al source targets are used instead of a single target. An electron beam is used to achieve well-controlled independent evaporation of the two elements. In a conventional low-pressure electron beam evaporation process, the resulting flux has a highly nonuniform composition. However, here we show that if an inert gas jet is used to entrain the two vapor plumes, gas phase interdiffusion can be sufficient to result in an almost fully homogenized vapor cloud that can then be transported and deposited on the substrate. This process is accomplished using a modified electron beam directed vapor deposition (EB-DVD) technique [25] and can be operated in a manner that facilitates non-line-of-sight deposition [26]. We find that the process results in high quality NiAl coatings with a composition that is easily manipulated by independently controlling the evaporation rate of each source. This is accomplished by modifying electron beam current density applied to each source to independently control its evaporation rate. We also investigate the effect of the deposition temperature upon the morphology of the coatings and show that deposition temperatures of about 1000 °C result in pore free, equiaxed grain structured coatings with a substrate interdiffusion zone that is small compared to the bond coatings thickness.

2. EB-DVD set up

The EB-DVD system used here is schematically illustrated in Fig. 3. It utilizes a rarefied, helium gas jet (created by supersonic expansion through a nozzle) to entrain atomically dispersed vapor created by electron beam evaporation. The (high velocity) inert gas jet atoms collide with those of the vapor and cause the vapor to be transported in the gas jet towards the substrate. Spreading of the evaporated flux can be impeded by the jet thereby causing high local vapor densities near the substrate. By matching the cross-section of the jet to that of the substrate, a large fraction of the vapor emitted by a source can be deposited on the substrate, resulting in high materials utilization efficiency and potentially high (>10 μm/min) deposition rates [27].

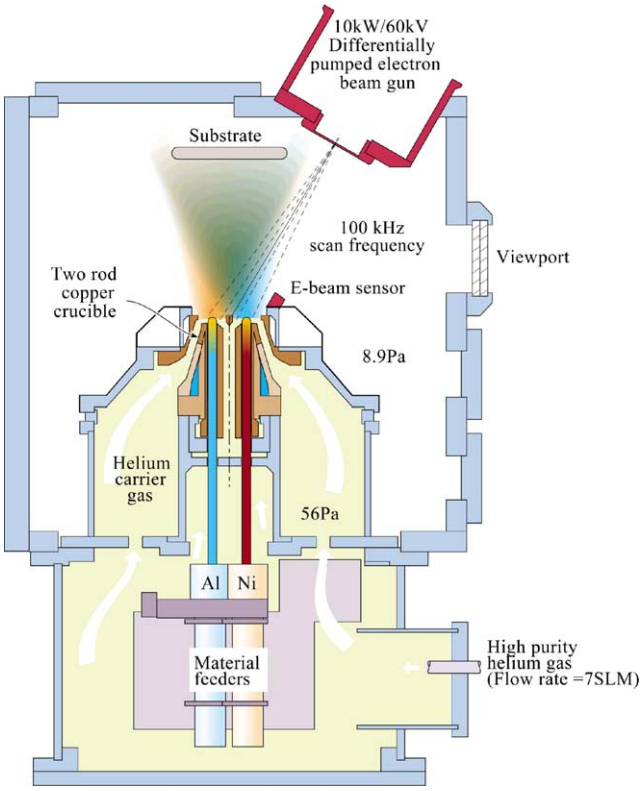

Fig. 3. Schematic illustration of the electron beam directed vapor deposition approach. A single electron beam can be scanned across up to four closely spaced metal sources.

Electron beam guns can evaporate a wide range of materials with high evaporation rate. This property makes the approach well suited for the fabrication of thick layers like bond coats. The EB-DVD approach uses a (differentially pumped) low vacuum, high voltage electron beam gun with a high beam scan frequency (up to 100 kHz) to melt the source materials. In order to co-evaporate nickel and aluminum sources with a single electron beam, the electron beam scan pattern was programmed to rapidly jump the electron beam between the two sources [28]. Each individual source material could be evaporated with different rates by controlling the dwell time of electron beam on each molten source pool. The ability to evaporate each individual source material with an independently controllable rate enabled a coating with precise composition to be synthesized. The two sources were positioned in the throat of a single gas jet creating nozzle as shown in Fig. 3. Gas phase scattering could then be used to mix the two vapor plums creating an almost homogeneous alloy vapor at the substrate.

To implement the approach, 99.99 at.% elemental nickel and aluminum rods with 0.32 mm diameter were used as the source materials. They were continuously raised during evaporation to compensate for evaporation. The two source rods were placed in separate crucibles as shown schematically in Fig. 4. In order to achieve an equiatomic composition, the electron beam dwell time (therefore the beams energy

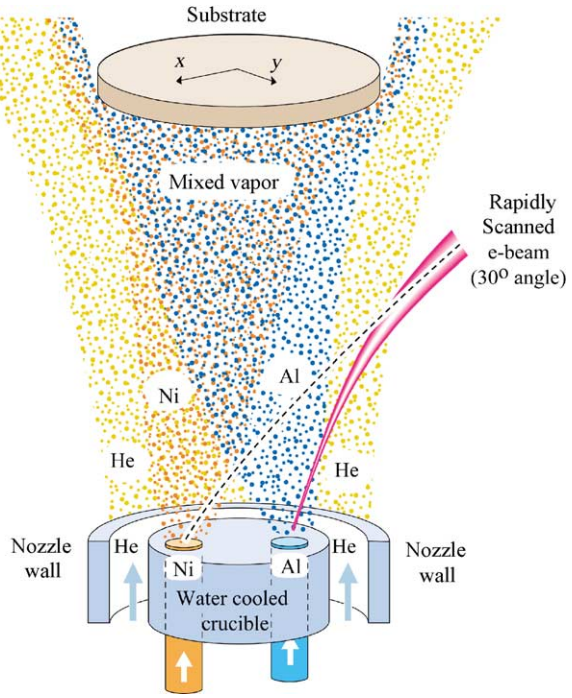

Fig. 4. Pure elemental nickel and aluminum materials are located in separate crucibles. They are co-evaporated and mix together in the vapor state before being directed by the helium carrier gas to the substrate.

splitting) applied on the nickel and aluminum source rods was set at the ratio of 39:61. The degree of vapor mixing was found to depend sensitively upon the properties of the gas jet flow. Direct simulation Monte Carlo (DSMC) simulations indicated that when the chamber pressure and the pressure ratio of the upstream/chamber were both relatively low, the lateral interdiffusion of the vapor atoms was increased and the vapor from two sources intermixed significantly during vapor phase transport [25]. Experimental trials conducted here indicated that adequate mixing could be achieved using an upstream pressure of 56 Pa and a chamber pressure of 8.9 Pa. For the annular nozzle used here (with an inner diameter of 30 mm), this corresponded to a He flow rate of 7 standard l/min (slm).

Commercial 25.4 mm diameter Hastelloy X coupons (provided by GE Aircraft Engines) were used as substrates for NiAl deposition. They had a 200 μm $Ni_{0.36}Co_{0.18}Cr_{0.16}Al_{0.29}Y_{0.005}$ coating on top to act as aluminum-contained substrates. The substrates were preheated to 450 °C for 1 h to clean the surface, and then heated to between 900 and 1100 °C for deposition. The deposition duration was 35 min and the average deposition rate was about 0.5–1 μm/min. After the deposition process, the samples were cooled to ambient within the chamber in the inert gas environment. Multiple synthesis methods including scanning electronic morphology (SEM), electron diffraction spectroscopy (EDS) and X-ray diffraction (XRD) were used to characterize the NiAl samples.

3. Experimental results

3.1. Structure and morphology

The cross-section morphology of the NiAl bond coat deposited at 1000 °C is shown in Fig. 5. The NiAl coating thickness was about 20 μm. The coating consisted of columnar grains with grain boundaries that extended completely across the coating. No pores were observed within the cross-section. EDS on the sample surface revealed a homogeneous coating layer consisting of 51 at.% of Ni and 49 at.% of Al, which indicated that the coating was in the single β-phase region of the Ni–Al binary phase diagram. A composition test along a randomly selected surface diameter gave a relative deviation of 1.2% over a 25 mm path.

The composition as a function of depth in the coating was measured using EDS on the sample's cross-section. The results indicated the as-coated NiAl layer had a uniform composition through the majority of the coating thickness, Fig. 6. A 7 μm interdiffusion zone was observed at the interface with the substrate. This interdiffusion zone was much smaller than that of NiAl diffusion coatings fabricated by solid-state aluminization methods [19,29]. Conventional diffusion coatings

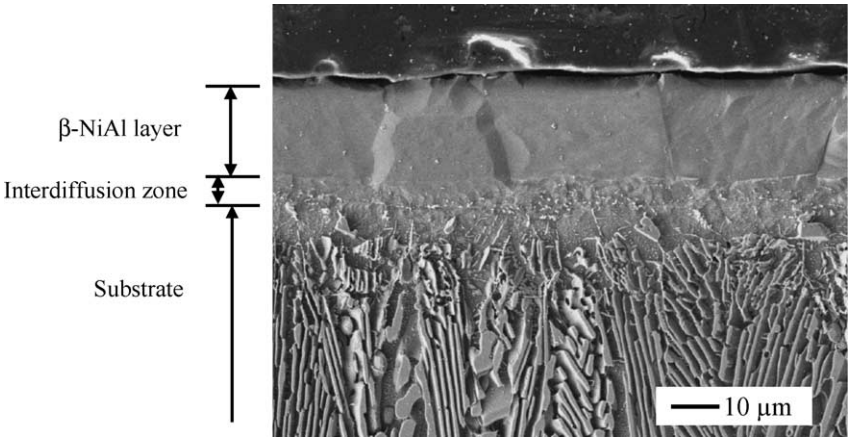

Fig. 5. SEM observation on the etched cross-section of a NiAl coating deposited at 1000 °C. The sample was etched in 5HCl:1HNO_3 for 10 s.

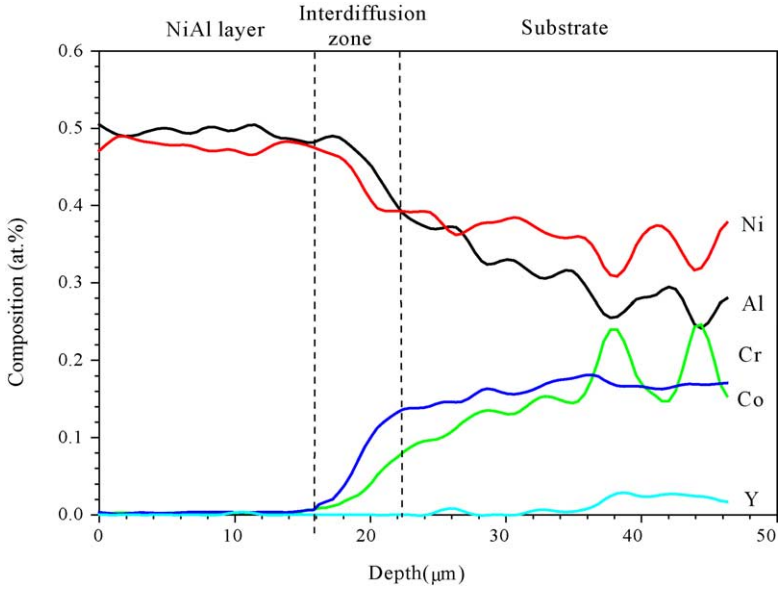

Fig. 6. The composition distribution on the cross-section of the NiAl coating deposited at 1000 °C.

contain an inner interdiffusion zone beneath the aluminide layer attributed to faster outward diffusion of nickel from the substrate surface region during aluminizing process. The typical interdiffusion zone thickness of the CVD made NiAl bond coat sample is about 20–25 μm [18,29]. In our sample, however, the diffusion distance was much less, and it is reasonable to conclude that the interface is relative sharp with no contamination of the coatings outer surface by substrate alloying or tramp impurity elements.

XRD analysis, Fig. 7, indicated that the NiAl coating was single β-phase. The intensity in the ⟨1 1 1⟩ and ⟨2 1 1⟩ directions were higher than the standard powder diffraction file. Analysis of X-ray pole figure data showed that the NiAl coatings were highly textured, with the majority of the grains having a surface normal parallel to the ⟨1 1 1⟩ direction, Fig. 8. This fiber texture has been frequently observed in metal polycrystalline thin films grown by PVD [30,31] and CVD methods [20].

The mechanism for the formation of these fiber textures is usually explained in terms of a grain evolutionary selection model proposed by Van der Drift [32,33]. In this model, fiber texture results from the difference in growth rates between different crystal faces of the grains on the surface of the film. Grains oriented with their faster growing directions perpendicular to the surface are preserved while slower growing grains are terminated as they intersect the column walls of taller grains [34].

The β-phase NiAl alloy has a similar growth texture to that reported for both nickel and aluminum, which have face centered cubic (fcc) structures. It often exhibits a ⟨1 1 1⟩ preferred orientation [35]. Since (1 1 1) faces in these crystal structures correspond to the most densely packed planes with the lowest energy, most of the grains in the coating layer thermodynamically prefer to be oriented such that their surface normal is

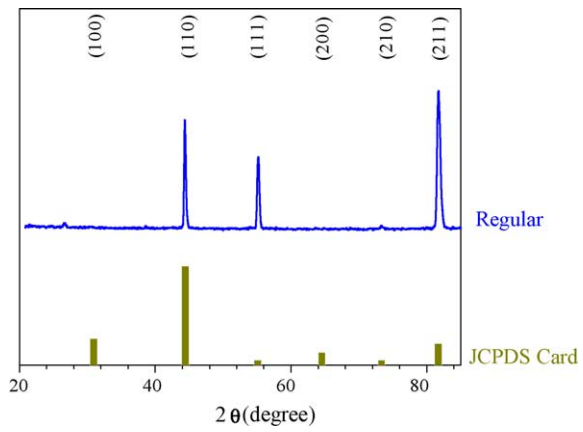

Fig. 7. XRD pattern of a NiAl bond coat deposited at 1000 °C and its comparison with the NiAl peaks given by JCPDS card.

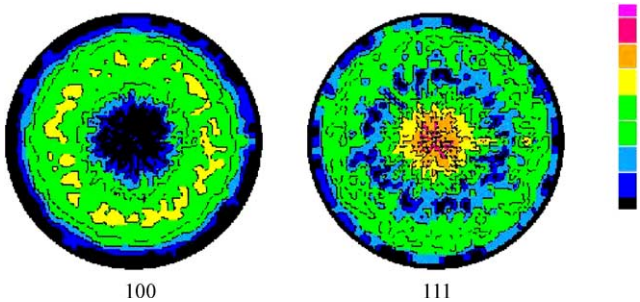

Fig. 8. X-ray pole figure analysis showed the NiAl coating layer was ⟨1 1 1⟩ direction textured. Note that each coaxial circle within the ring represents an angle between the sample surface and the specified crystal orientation. The angle decreases continuously along any radius with the center of the ring representing 90° and the edge representing 0°.

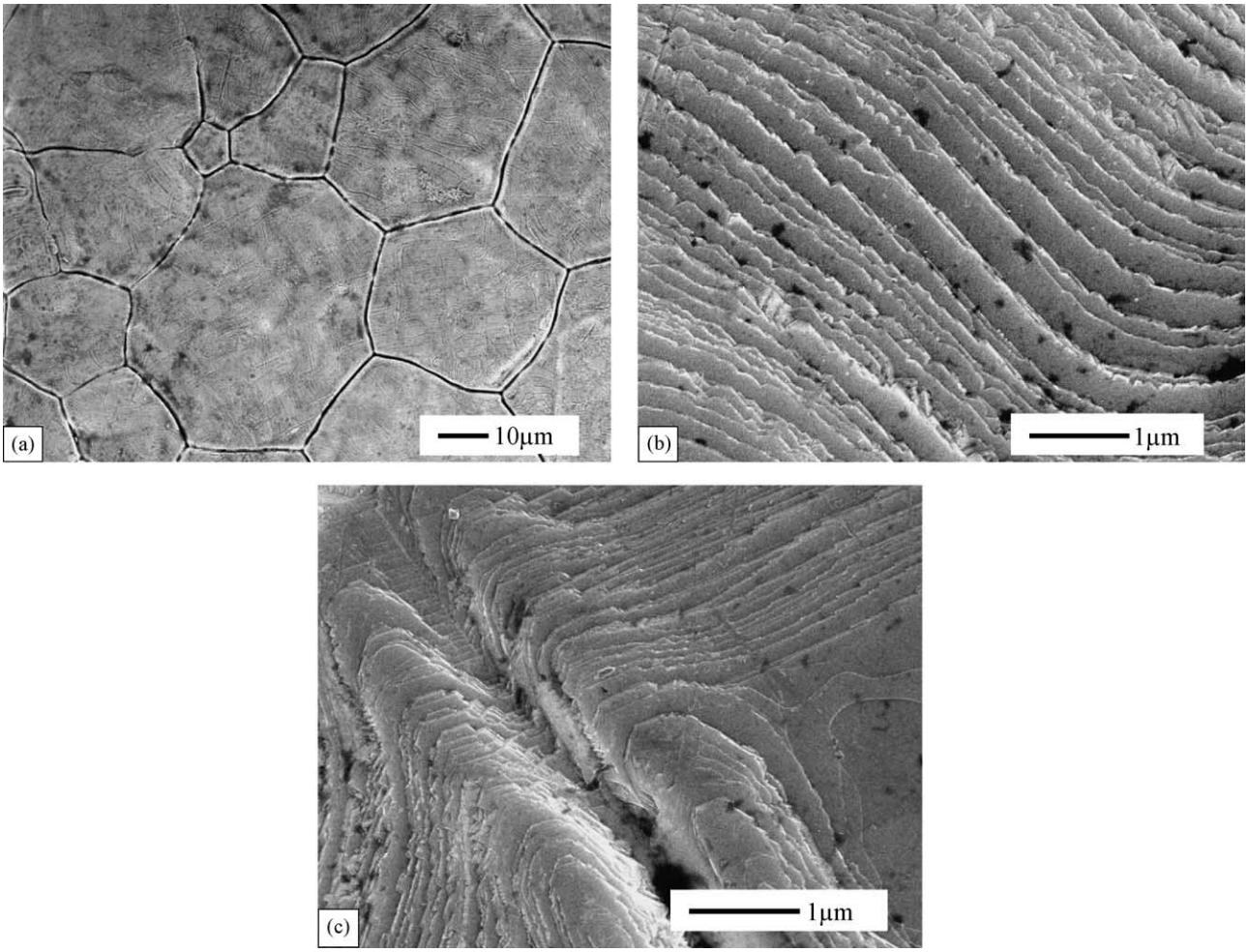

Fig. 9. Surface morphologies of NiAl alloys deposited at 1000 °C: (a) NiAl surface consists of crystalline grains with grain size 10–50 μm; (b) high magnification image; (c) the strikes change their direction and twist at the grain boundary.

perpendicular to these highest density planes [32,36]. This interpretation is consistent with the observations in the X-ray pole figure.

The surface morphology of a NiAl coating deposited at 1000 °C is shown in Fig. 9. The as-deposited NiAl surface consisted of relatively large roughly equiaxed crystalline grains with an average grain size of 30 μm, Fig. 9(a). At high magnification, Fig. 9(b), the surface of each grain had a terraced substructure. The terraces changed direction and angle at the grain boundary, forming prominent ridges on either side of the grain boundary and a shallow groove between them, Fig. 9(c). The terraced surface is consistent with the growth terraces frequently observed on vapor deposited nickel surfaces though in the NiAl case they appear to be many atomic layers thick [37].

3.2. Temperature effects

Growth studies revealed that the coatings morphology was affected by many factors, including deposition rate, growth chamber pressure, elemental composition of the depositing atoms, substrate temperature, and even the deposit thickness [38–41]. To study how the substrate temperature affected the NiAl coating, three samples were deposited at different temperatures (900, 1000 and 1100 °C, respectively), but with otherwise identical process conditions to those reported above.

Fig. 10 shows SEM secondary electron images of the three NiAl coating surfaces. Cross-sectional images and composition profiles are shown in Fig. 11. From the surface images, we observed that the grains of the sample deposited at 900 °C, Fig. 10(a), had a relatively small average diameter of 10–20 μm. Deep grooves and small voids were observed in the surface of the grains. Cross-sectional images, Fig. 11(a), indicated that these voids were shallow and did not penetrate far into the coating. These observations are consistent with flux shadowing of the growth surface, which at 900 °C and a deposition rate of 1 μm/min appears not to be fully compensated by lateral surface diffusion [42].

Increasing the deposition temperature to 1000 °C significantly reduced both the grain boundary grooves and the grain

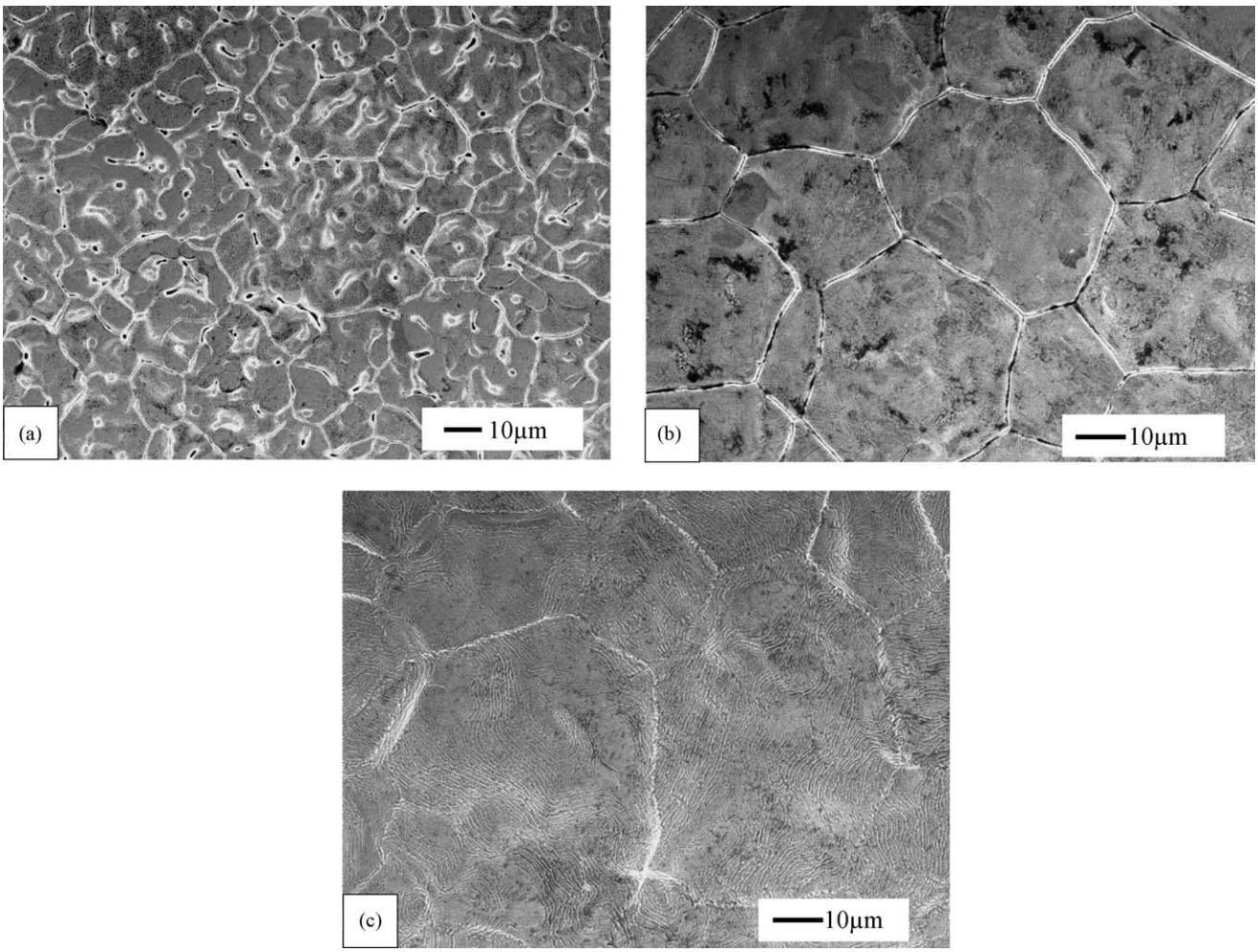

Fig. 10. SEM surface morphologies of NiAl alloys deposited at different temperatures: (a) sample deposited at 900 °C; (b) sample deposited at 1000 °C; (c) sample deposited at 1100 °C.

interior surface pores, Fig. 10(b). The average grain size also increased to 30 μm. These changes are consistent with a higher adatom surface mobility. Like the sample deposited at 900 °C, interdiffusion with the substrate was limited to a narrow region at the coating layer/substrate interface and nickel/aluminum concentrations were uniform along coating layer depth in the EDS cross-section observation, Fig. 11(b).

Further increase of the substrate temperature to 1100 °C resulted in further changes to the sample surface. The average grain size increased to 35 μm and instead of the sharp grain boundary grooves that were observed in NiAl samples grown at 900 and 1000 °C, wide prominent ridges were formed at the grain boundaries, Fig. 10(c). Significant elemental interdiffusion was found at the interface of the 1100 °C deposited sample. It included both diffusion of Ni and Al inner ward and Cr and Co outward, Fig. 11(c). The diffusion distances of the elements were longer than 15 μm.

We also observed that the substrate temperature affected terraced substructure of NiAl coating surface. To be more specific, we found that the terrace density decreased with increase of the substrate temperature. For the sample deposited at 1000 °C, the terrace density was about 7 μm^{-1}, Fig. 9(b). However, the terrace density decreased to about 2 μm^{-1} as the substrate temperature was increased to 1100 °C, Fig. 12.

It is commonly accepted that one of the most important factors controlling the growth mode is the Ehrlich–Schwoebel (ES) energy barrier for diffusing adatoms at descending step edges [43,44]. When this is high compared to that for on-terrace migration step flow growth is impeded and the terrace edge density increases. Our observations suggest that this is the situation here. At high temperature, thermal activation of the adatoms increases the probability of overcoming the ES barrier at the terrace step, leading to a smoother surface mode of growth.

The formation of grain boundary grooves at 1000 °C in Fig. 9(c) and the voids at 900 °C in Fig. 10(a) can also be explained similarly. Grain boundaries, where the grains change crystal orientations, can be considered as energy barriers against the diffusion of adatoms. At 1000 °C, the adatoms are

not activated enough to pass through the grain boundaries and accumulate on each side of them, thus forming the prominent ridges and then grooves in between. At lower temperature such as 900 °C, the adatoms cannot even obtain enough energy for lateral diffusion within the grain surface, leading to the formation of voids on the surface.

4. Discussion

The experimental results suggest that EB-DVD is an effective technique for the deposition of fully dense, homogenous, β-NiAl coatings. The coating composition can be preselected by simply controlling the electron beam residence

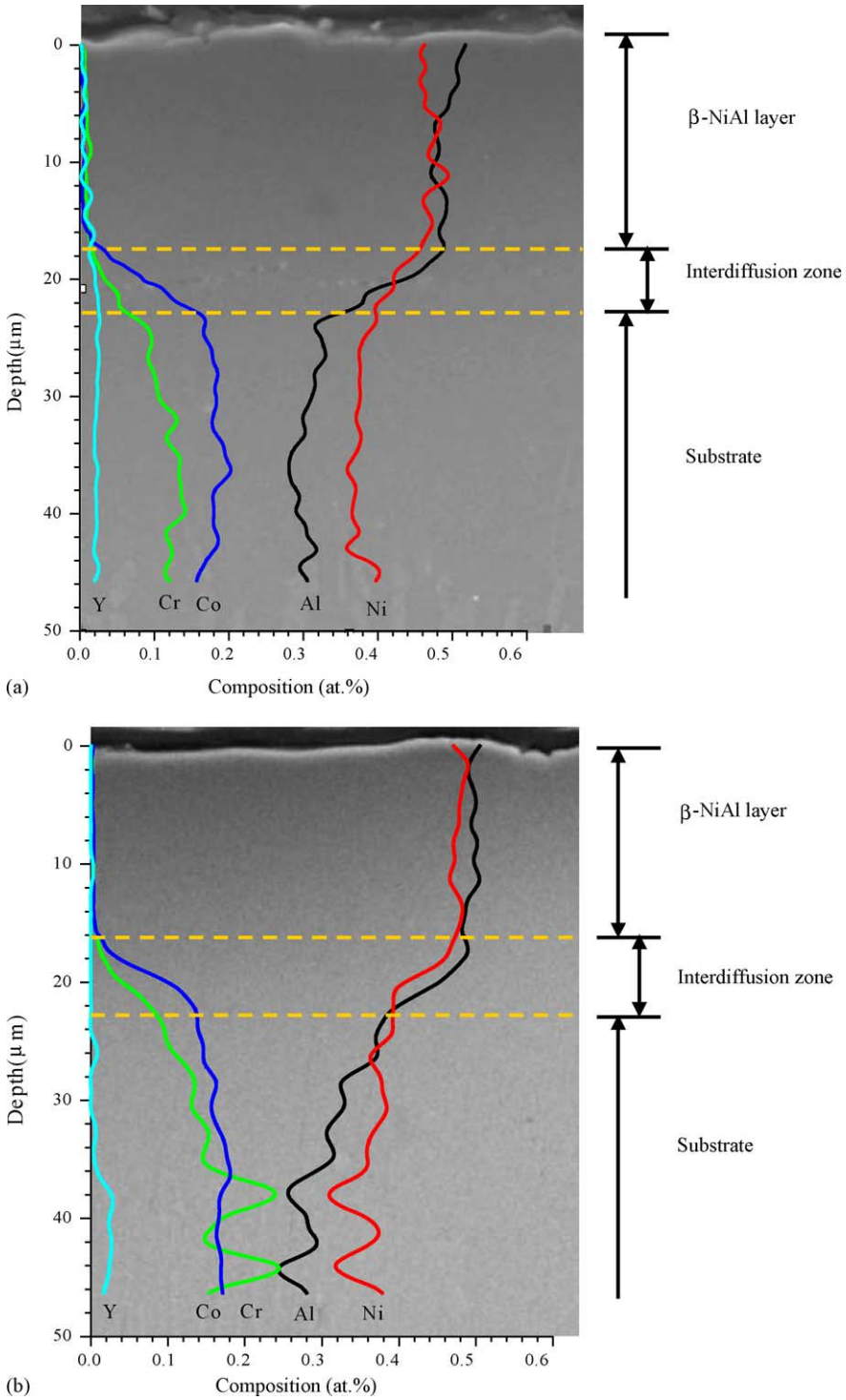

Fig. 11. SEM/EDS cross-section observation of three NiAl samples deposited at different temperatures: (a) sample deposited at 900 °C; (b) sample deposited at 1000 °C; (c) sample deposited at 1100 °C.

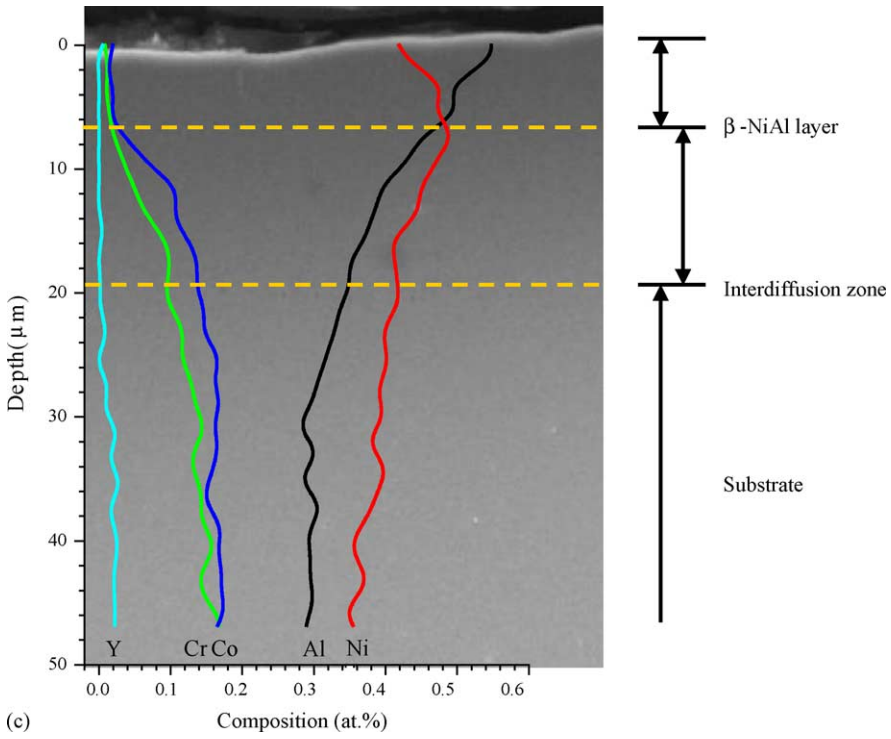

Fig. 11. (*Continued*).

time on each melt source pool. No penetrating voids were observed in the NiAl coating layers grown at temperatures between 900 and 1100 °C. The NiAl bond coats deposited using EB-DVD are rather different to those made by other fabricating methods. Since outward diffusion of elements from the substrate was greatly mitigated at deposition temperatures of 1000 °C and below, only a small interdiffusion zone was formed beneath EB-DVD deposited NiAl bond coat layer.

It is believed that the durability of current TBC system relies on the strong bonding between the TGO and the bond coat. A creep-resistant bond coat with a flat surface is desirable to reduce the out-of-plane tensile stress across the TGO/bond coat interface and the diffusion of deleterious elements such as W, Ti, Ta, or S, should be prevented to maintain a strong bond [4]. The rate of growth of the TGO layer also depends upon the oxides grain size, which may be linked to that of the bond coat. Thus the ideal bond coat layer should have a flat surface, a large grain size and minimal surface contamination by deleterious substrate alloy elements [19,20,45]. The EB-DVD approach appears to have the flexibility to be adjusted to modify bond coats properties with provisos. For example our experiments indicate that samples grown at high substrate temperatures of 1100 °C have relative large grain sizes and flat surfaces. However, high temperature deposition also enables elemental diffusion between the bond coat layer and the substrate, providing opportunities for the migration of deleterious elements that might degrade the bond coat/TGO adhesion [18,46].

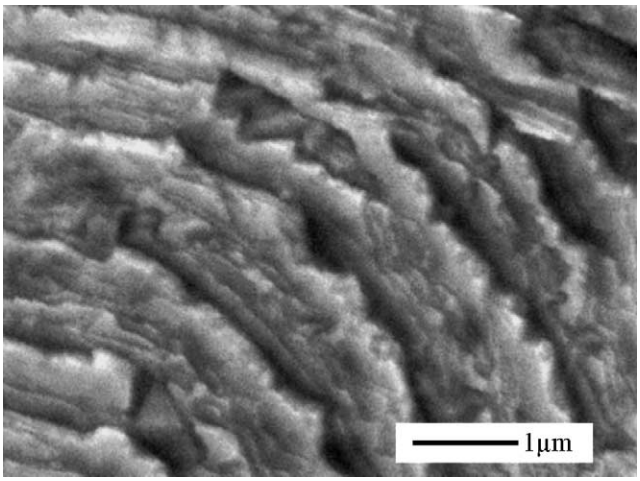

Fig. 12. High magnification SEM surface image of NiAl alloys deposited at 1100 °C.

Decreasing the substrate temperature to 1000 °C avoided the elemental diffusion problem and resulted in a sharper bond coat/substrate interfaces. Reducing the substrate temperature further (to 900 °C) was not found to be beneficial since the coating surface then became rough and voids started to appear. If used unmodified in a TBC system, such an undulating surface bond coat will result in an undulated bond coat/TGO interface, which have been linked to reduced spallation lifetimes [4,19]. The experiments reported here indicate the best substrate temperature for an EB-DVD NiAl bond coat is likely to be 1000 °C though lower optimal

temperatures might be possible using ion-assisted deposition to increase surface mobility without interdiffusion of underlying layers.

The oxidation of NiAl is significantly reduced by the addition of platinum to NiAl coatings. Several research groups in this field have also demonstrated that the addition of small quantities of reactive elements or solute/precipitation strengthening dopants such as Hf, Y, Zr, and Cr can improve hot corrosion and oxidation resistance of NiAl bond coats [1,4]. The EB-DVD approach used here could be used to evaporate up to four material (either elemental or alloy) sources. It may therefore be possible to extent the approach to incorporate ternary and quaternary additions to the NiAl system.

5. Conclusions

We have utilized an EB-DVD technique to deposit NiAl bond coats. By adjusting the electron beam dwell time on individual source materials and the inert gas jet flow field, homogeneous, pore free NiAl coating layers are fabricated without the assistance of post-deposition heat treatments. Coating layers with a single β-phase structure and no surface contamination with substrate alloy elements can be fabricated. The extent of the coating–substrate interdiffusion and the coatings smoothness and grain size are all shown to depend upon the temperature selected for deposition. Deposition temperatures of about 1000 °C appear optimal for the deposition of bond coats intended for use in thermal barrier coating systems.

Acknowledgements

We would like to thank Profs. Carlos Levi, Anthony Evans and David Clarke of the University of California, Santa Barbara for useful comments, and Dr. David Wortman, GE Corporate R&D, Schenectady, New York, for providing substrates and helpful discussions. We are grateful to Dr. Steve Fishman of the Office of Naval Research for support of this work through ONR Contract No. N00014-00-1-0438.

References

[1] C.G. Levi, Curr. Opin. Solid State Mater. 8 (2004) 77.
[2] D.R. Clarke, C.G. Levi, Ann. Rev. Mater. Res. 33 (2003) 383.
[3] M.R. Brickey, J.L. Lee, Oxidation Met. 54 (2000) 237.
[4] N.P. Padture, M. Gell, E.H. Jordan, Science 296 (2002) 280.
[5] M.J. Stiger, N.M. Yanar, M.G. Topping, F.S. Pettit, G.H. Meier, Z. Metallkd. 90 (1999) 1069.
[6] R. Darolia, JOM 43 (1991) 44.
[7] W.S. Walston, R. Darolia, D.A. Demania, Mater. Sci. Eng. A 239 (1997) 353.
[8] D.B. Miracle, Acta Metall. Mater. 41 (1993) 649.
[9] R.D. Noebe, R.R. Bowman, M.V. Nathal, Int. Mater. Rev. 38 (1993) 193.
[10] R. Mevrel, C. Duret, R. Pichoir, Mater. Sci. Technol. 2 (1986) 201.
[11] S.R. Choi, J.W. Hutchinson, A.G. Evans, Mech. Mater. 31 (1999) 447.
[12] J. Angenete, K. Stiller, Mater. Sci. Eng. A 316 (2001) 182.
[13] E.G. Colgan, Mater. Sci. Rep. 5 (1990) 1.
[14] E. Ma, C.V. Thompson, L.A. Clevenger, J. Appl. Phys. 69 (1991) 2211.
[15] K. Barmak, C. Michaelen, G. Lucadamo, J. Mater. Res. 12 (1997) 133.
[16] A.E. Edelstein, R.K. Everett, G.R. Richardson, S.B. Qadri, J.C. Foley, J.H. Perepezko, Mater. Sci. Eng. A 195 (1995) 13.
[17] B.M. Warnes, D.C. Punola, Surf. Coat. Technol. 94–95 (1997) 1.
[18] W.Y. Lee, Y. Zhang, I.G. Wright, B.A. Pint, P.K. Liaw, Metall. Trans. A 29A (1998) 833.
[19] J.A. Haynes, Y. Zhang, W.Y. Lee, B.A. Pint, I.G. Wright, K.M. Cooley, Elevated Temp. Coat.: Sci. Technol. III 185 (1999).
[20] Y. Zhang, W.Y. Lee, J.A. Haynes, I.G. Wright, B.A. Pint, K.M. Cooley, P.K. Liaw, Metall. Mater. Trans. A 30 (1999) 2679.
[21] L.L. Lee, D.E. Laughlin, D.N. Lambeth, IEEE Trans. Magn. 31 (1995) 2728.
[22] A.T. Alpas, Y. Ding, Y. Zhang, D.O. Northwood, Surf. Coat. Technol. 94–95 (1997) 483.
[23] D. Zhong, J.J. Moore, J. Disam, S. Thiel, I. Dahan, Surf. Coat. Technol. 120–121 (1999) 22.
[24] J.L. He, C.H. Yu, A. Leyland, A.D. Wilson, A. Matthews, Surf. Coat. Technol. 155 (2002) 67.
[25] D.D. Hass, K. Dharmasena, H.N.G. Wadley, Proceedings of the International Conference on High-power Electron Beam Technology, October 27–29, 2002, p. 8-1.
[26] D.D. Hass, Y. Marciano, H.N.G. Wadley, Surf. Coat. Technol. 185 (2004) 283.
[27] J.F. Groves, H.N.G. Wadley, Composites, Part B 28B (1997) 57.
[28] U. Schulz, K. Fritscher, C. Leyens, Surf. Coat. Technol. 133–134 (2002) 40.
[29] B. Ning, M.E. Stevenson, M.L. Weaver, R.C. Bradt, Surf. Coat. Technol. 163–164 (2003) 112.
[30] D.B. Knorr, D.P. Tracy, Appl. Phys. Lett. 59 (1991) 3241.
[31] L. Tang, G. Thomas, J. Appl. Phys. 74 (1993) 5025.
[32] Van der Drift, Philips Res. Rep. 22 (1967) 267.
[33] M.B. Stearns, C.H. Lee, C.-H. Chang, A.K. Petford-Long, in: M. Hong, S. Wolf, C.C. Gubser (Eds.), Metallic Multilayers and Epitaxy, TMS, Warrendale, PA, 1988, p. 55.
[34] F. Ying, R.W. Smith, D.J. Srolovitz, Appl. Phys. Lett. 69 (1996) 3007.
[35] D.B. Knorr, D.P. Tracy, Appl. Phys. Lett. 59 (1991) 3241.
[36] L. Dong, D.J. Srolovitz, J. Appl. Phys. 84 (1998) 5261.
[37] P. Gambardella, K. Kern, Surf. Sci. 475 (2001) L229.
[38] K.-H. Müller, J. Appl. Phys. 58 (1985) 2573.
[39] B.V. Movchan, A.V. Demchishin, Phys. Met. Metallogr. 28 (1969) 83.
[40] K. Kennedy, Proceedings of the AVS Vacuum Metallurgical Conference, Los Angeles, 1968, p. 195.
[41] J.A. Thornton, J. Vac. Sci. Technol. 12 (1975) 830.
[42] D.D. Hass, Y.G. Yang, H.N.G. Wadley, Surf. Coat. Technol., submitted for publication.
[43] V.I. Trofimov, V.G. Mokervo, Mater. Sci. Eng. B 89 (2002) 420.
[44] J. Wollschlager, M. Bierkandt, M.I. Larsson, Appl. Surf. Sci. 219 (2003) 107.
[45] B.A. Pint, I.G. Wright, W.Y. Lee, et al., Mater. Sci. Eng. A 245 (1998) 201.
[46] J.G. Smeggil, Mater. Sci. Eng. A 87 (1987) 261.